Applied Chemical Engineering (2025) Volume 8 Issue 3 ISSN: 2578-2010 (O)
doi: 10.59429/ace.v8i3.5715

ORIGINAL RESEARCH ARTICLE

Sustainable activated carbon from corn cob for efficient removal of methyl orange and methyl red from water

Hani Mueen[1], Thuraya A. Abdul Hussian[2], Haider Falih Shamikh Al-Saedi[3], Kareem Al-Adily[4], Shaker Salem[5], Safa Sabri[6], Talib Munshid Hanoon[7], Basim Mohammed Saadi[8*]

[1] *Department of Nursing, Al-Zahrawi University College, Karbala, Iraq*
[2] *Department of nuclear physics and environment, Al-Turath University, Iraq*
[3] *Faculty of pharmacy, department of pharmaceutic, University of Al-Ameed, Iraq*
[4] *Applied and Mechanical Engineering, Al-Hadi University College, Baghdad, 10011. Iraq*
[5] *department of medical engineering, University of Manara, (Maysan), Iraq*
[6] *department of medical engineering, Warka University College, Iraq*
[7] *Mazaya university college, Iraq*
[8] *Department of Medical Laboratories Technology, Al-Nisour University College, Nisour Seq. Karkh, Baghdad, Iraq*
***Corresponding author:** Basim Mohammed Saadi; basimsaadi51@gmail.com

ABSTRACT

This study reports the synthesis of activated carbon from corncob biomass via hydrochloric-acid chemical activation (HCl). The resulting bio-based activated carbon was subsequently evaluated as an efficient adsorbent for the aqueous-phase removal of model synthetic azo dyes—methyl orange (MO) and methyl red (MR). The physicochemical and morphological characteristics of the activated carbon were examined using Scanning Electron Microscopy (SEM) and Transmission Electron Microscopy (TEM). The effects of key operational parameters, including adsorbent dosage, initial dye concentration, and temperature, were systematically investigated. The results indicated that the corn cob-based activated carbon exhibited a favorable surface morphology, relatively high surface area, and significant dye removal efficiency. MR showed better adsorption performance than MO, which can be attributed to differences in molecular structure, ionic properties, and specific interactions with surface functional groups on the activated carbon. Opposite-charge attraction and π–π stacking with the carbon surface boosted adsorption, most notably for MR. An increase in adsorbent dosage led to higher dye removal percentages due to more available binding sites; however, the adsorption capacity per unit mass (qe) decreased at higher doses, likely due to particle agglomeration and reduced effective surface area. These findings suggest that corn cob-derived activated carbon is a promising low-cost, environmentally friendly adsorbent for wastewater treatment applications.

Keywords: Removal; Corn Cob; Activated Carbon; Methyl orange (MO); Methyl red (MR)

ARTICLE INFO

Received: 1 August 2025
Accepted: 5 September 2025
Available online: 12 September 2025

1. Introduction

Environmental contamination is one of the most pressing problems of the contemporary world, and water pollution is of prime concern due to its direct effects on human health, aquatic life, and agricultural productivity. Rapid industrialization, urban expansion, and improper waste disposal, have intensified freshwater pollution. Heavy metals, pharmaceuticals and synthetic organic compounds are currently often found in rivers, lakes, and in underground water. These pollutants not only deteriorate water quality but also disrupt the ecological balance and pose long-term hazards to public health and biodiversity[1-4].

Among various water pollutants, synthetic dyes pose great concern, as they are applied widely in the textile, paper, plastic and cosmetic industries. Dyes such as methyl orange, methylene blue, and methyl red are soluble, chemically stable, and resistant to biodegradation. Dyestuffs may cause intense colourations in water bodies and might reduce light penetration and influence the photosynthesis of aquatic plants already at low concentrations. Moreover, most dyes and their degradation products are toxic, mutagenic, or carcinogenic, making their removal from industrial wastewaters a priority before subsequent release to the environment[5-8].

Adsorption is known to be an efficient and useful technique used in the removal of dyes in addition to other organic pollutants from wastewater. This procedure presents many benefits including its low expense, simple operation, high efficiency in low concentrations, and the possibility of adsorbent regeneration and recycling. Adsorbents are classified as activated carbon (AC), natural clays, zeolites, synthetic resins and metal–organic frameworks (MOFs). Of these, activated carbon is still the most commonly used because of its high surface area, highly developed porosity, and excellent ability to adsorb a wide variety of contaminants. Nonetheless, the high cost of production has led to extensive work toward environmentally sustainable and low-cost alternatives[4, 9, 10].

In recent years, the usage of agro-wastes as precursors in the preparation of activated carbon has become very popular. should be corrected to Solid wastes of organic origin, such as discarded corn cobs, rice hulls, coconut shells, sawdust, and sugarcane bagasse, can be converted into activated carbon through physical or chemical activation.[11-13]. The bio-adsorbents described in these studies therefore provide a low-cost, renewable, alternative to commercial activated carbon and encourage waste valorization and a circular economy. Agricultural residue-based activated carbon also performs equally well, when characterized properly, in the adsorption ability, particularly, dyes and other recalcitrant pollutants from the waste discharge. This system is not only dealing with environmental pollution but is also contributing to integrated resource conservation[14-17].

In this study, activated carbon derived from corn cob biomass was successfully prepared using hydrochloric acid activation and applied as an effective adsorbent for removing synthetic dyes from aqueous solutions. The characterization results confirmed that the bio-based activated carbon possesses favorable surface morphology and porosity, which contribute to its high adsorption efficiency. The adsorption behavior was influenced by key operational parameters such as adsorbent dosage, dye concentration, and temperature, demonstrating the material's sensitivity and adaptability to different treatment conditions. Overall, the findings highlight the potential of agricultural waste valorization in producing low-cost and environmentally friendly adsorbents for water purification applications. The use of corn cobs as a precursor not only provides a sustainable solution for biomass disposal, but also contributes to the development of circular economy practices in environmental remediation. Future research should focus on scaling up the production process, optimizing regeneration cycles, and exploring the adsorbent's efficiency against other classes of pollutants.

2. Experimental part

2.1. Preparation of corn crab biomass into activated carbon

Corn cob materials were collected and then washed repeatedly with deionised water to remove dirt and impurities; the corn biomass was air-dried for 48 h at room temperature. The dried biomass was chopped into small pieces, oven-dried at 105 °C for 24 h to remove residual moisture, milled, and passed through a sieve to obtain particles of consistent size (approximately 0.5–1.0 mm). Chemical activation was performed by impregnating the biomass with hydrochloric acid (HCl) at a 1:1 w/v biomass:HCl ratio. The slurry was stirred at room temperature for 2 h and soaked for 24 h to ensure complete penetration of the activating reagent. After HCl impregnation, the precursor was briefly rinsed to remove free acid liquor, oven-dried at 105 °C to constant weight to standardize the dry mass, and subsequently carbonized (final step). Carbonization was conducted at 500 °C for 2 h in an inert N_2 atmosphere to prevent oxidation. After synthesis, the carbonised product was cooled to room temperature, washed several times with distilled water to neutral pH, and dried at 110 °C for 12 h. The final product—corn-cob-derived HCl-activated carbon—was sealed for sample characterisation and adsorption studies. As shown in Figure 1, the process flow for preparing HCl-activated carbon from corn cobs is illustrated (washing → drying → size reduction → acid impregnation → pre-drying → carbonization at 500 °C under N_2 → post-washing → final drying). Operational details for reproducibility: HCl concentration was 1.0 M; the heating rate during carbonization was 10 °C min^{-1}; nitrogen flow was maintained at 150 mL min^{-1} throughout the purge and hold stages. The post-synthesis washing protocol consisted of three hot-wash cycles with distilled water at 60 ± 5 °C (solid:liquid ≈ 1:20 w/v), followed by room-temperature distilled-water rinses until the filtrate reached pH 6.8–7.2 and tested negative for chloride ($AgNO_3$ test). The washed solid was then oven-dried at 110 °C for 12 h before storage.

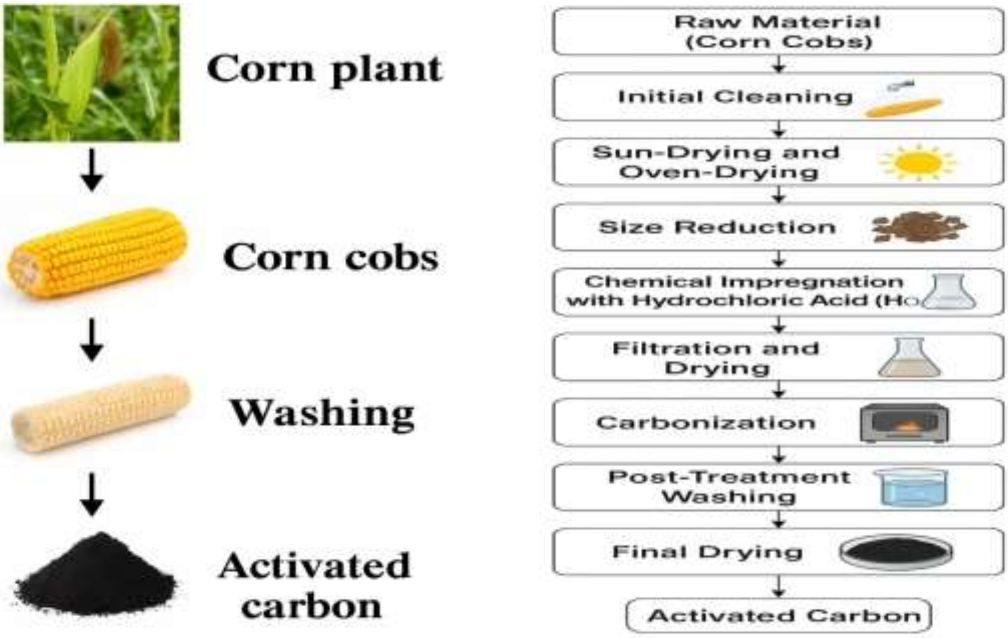

Figure 1. Preparation of corn crab biomass into activated carbon

2.2. Adsorption study

Batch adsorption tests were conducted in 10 mL Erlenmeyer flasks containing 100 mL of dye solution with initial concentrations $C_0 = 10\text{–}100\ mg\cdot L^{-1}$ (MO/MR), at 25 ± 0.5 °C in a thermostated orbital shaker. The pH was adjusted to 6.0 ± 0.1 with 0.01 M HCl/NaOH (buffer used where specified). The adsorbent dose was 0.05 g, and agitation was set to 150 rpm. Kinetic runs used $C_0 = 50\ mg\cdot L^{-1}$ over 0–60 min; isotherms used $C_0 = 10\text{–}100\ mg\cdot L^{-1}$ at 15-45 °C. At set intervals, 5 mL aliquots were withdrawn, filtered, and analyzed by UV–Vis at the dye's λmax using calibration curves. The dye percentage removal (E%), adsorption capacity (Qe, mg/g), were determined using Equations.

$$E\%=\frac{C_o\text{-}C_e}{C_o}\times100 \quad (1)$$

$$Q_e(\frac{mg}{g})=\frac{(C_o\text{-}C_e)V(ml)}{m(g)} \quad (2)$$

3. Result and discussion

The surface morphology of hydrochloric acid-activated carbon prepared from corn cobs can be observed in its SEM image at 10,000 magnification, as shown in Figure 2a. The sample's carbon particles exhibit a coarse morphology, characterized by appreciable The material has varying thicknesses, irregular flanges and fringes, and sharply angular edges. These morphological characteristics are signs of effective chemical activation, which in turn favors the formation of porosity through the release of volatile species and expansion of the carbon structure. Apparent surface cracks and gaps reflect dehydration and acid-catalyzed decomposition inherent to HCl-assisted carbonization. In addition to this, the dispersed fine debris and intercalated structures indicate an increased surface area, which would be favourable for adsorption uptake. It is evident from the SEM micrograph that the porous structure of the material is appropriate to favour good dye uptake from aqueous solution[18, 19].

Figure 2b shows SEM micrographs of the activated carbon surface after exposure to methyl red (MR). Relative to the pristine material, the post-adsorption surface exhibits locally smoother regions with agglomerated particulate deposits and occasional film-like overlayers attributable to dye accumulation. Several cracks and pore mouths appear partially occluded, and sharp edges are less distinct, consistent with pore filling and surface coverage. The presence of irregular aggregates and roughened textures suggests predominantly physical adsorption, with possible electrostatic interactions between the dye and the carbon surface. Collectively, these morphological changes are consistent with MR uptake by the activated carbon [16, 20, 21].

Figure 2c presents SEM micrographs of the activated carbon following methyl orange (MO) adsorption. Relative to the unloaded adsorbent, the surface is partly covered by a thin, discontinuous overlayer attributable to dye deposition. This coating obscures portions of the original roughness and pore mouths, indicating surface coverage and partial pore blocking at adsorption sites. Aggregated particles coexisting with locally smoother regions suggest dye–carbon complex formation, plausibly mediated by electrostatic attraction and π–π stacking with graphitic domains. Compared with the MR-loaded surface, MO yields a more dispersed deposition with fewer dense clusters. The SEM features—a thin film-like overlayer, dispersed aggregates, and partial pore-mouth occlusion—are consistent with surface coverage by MO on the activated carbon [22].

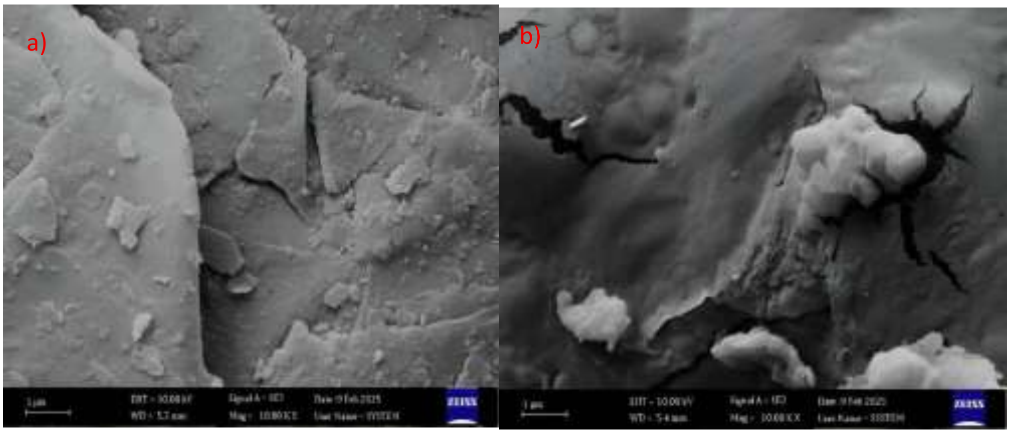

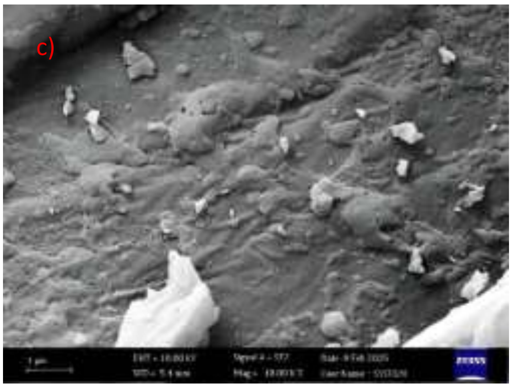

Figure 2. FESEM image of a) Activated carbon , b) activated carbon after methyl red (MR) , c) the activated carbon surface following methyl orange (MO)

TEM micrographs reveal an irregular, interconnected network of carbon particles with frequent necking between adjacent domains, indicative of an aggregated, porous morphology. The scale bar (60 nm, 100 nm) indicates the successful formation of nanometer-scale features upon activation and carbonisation (Figure 3). The contrast for the electron-dense features is not uniform (variable), suggesting that they have a non-homogeneous internal structure as well as possibly different crystallinity or density throughout the sample. The long-bent morphologies may be associated with folded or disordered graphene-like sheets, usually found in chemically activated bio-based AC[23]. The observed morphology—irregular, interconnected pores consistent with high surface area—facilitates adsorption by providing abundant accessible sites. This nanoscale surface texture is beneficial for the dye molecules' interaction with the material through a large number of surface-active sites [24, 25].

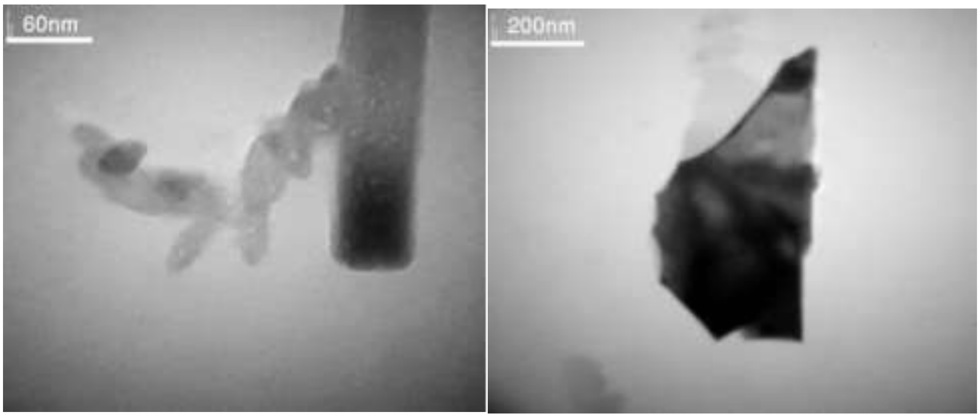

Figure 3. TEM image of activated carbon

3.1. Effect of the amount of adsorbent dosage

The influence of the amount of adsorbent on the removal percentage of methyl orange (MO) and methyl red (MR) dyes was investigated in the range of 0.01–0.12 g of activated carbon prepared from corn cobs at room temperature (Figure 4). The results showed a considerable increase in removal percentage for both dyes with increasing adsorbent dosage. This enhancement is primarily due to the provision of more active surface sites and a larger surface area resulting from the increased amount of adsorbent, which promotes better contact between dye molecules and the carbon surface[26, 27]. However, simultaneously, the adsorption capacity per unit mass (qe, mg/g) decreased dramatically as the adsorbent dosage increased. This negative relationship is typically attributed to the agglomeration of adsorbent particles at high dosages, which results in a decrease in the available surface area, rendering only a portion of the adsorption sites functional. Moreover, at high doses, the constant quantity of dye molecules is no longer sufficient to fill all active sites, resulting in decreased adsorption efficiency per gram of adsorbent. These observations are the same for both

MO and MR dyes, where the difference in adsorption behaviour can be attributed to the change in molecular structure and preference with the activated carbon surface[28].

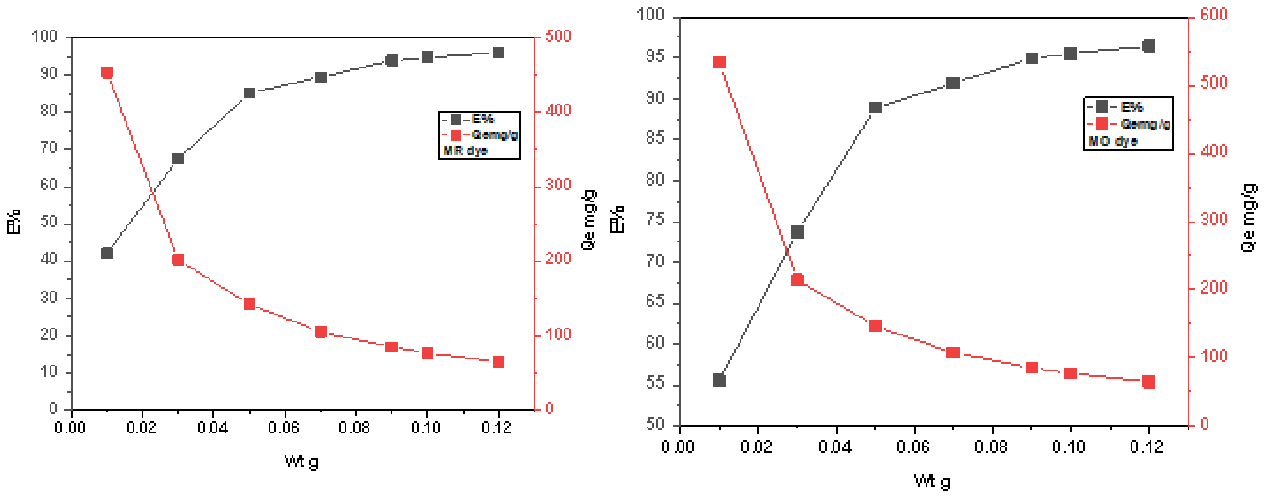

Figure 4. Effect of the amount of the adsorbent on the removal percentage of methyl orange (MO) and methyl red (MR) dyes

3.2. The initial concentration influence on the adsorptive performance

They studied the effect of initial dye concentration on the adsorption of MO and MR onto activated carbon prepared from corn cobs, covering the range of [insert range, for example, 10–100 mg/L Figure 5. The findings also indicated that the total removal percentage decreased with the rise in the initial concentration of the dye, but the adsorption capacity (qe, mg/g) was higher for both dyes. This is often due to the complete blockage of the adsorbent's active sites. At lower concentrations of the dyes, the relative abundance of adsorption sites compared to the dye molecules led to a high proportion of dye molecules being effectively captured (i.e., taking maximum advantage of the available adsorption sites), which is reflected in the high percentage removal[29]. But when more and more dye molecules are present, the active sites are already saturated with dye, and the removal efficiency decreases. However, the adsorption amount per unit mass of adsorbent (qe) is greater at a higher dye concentration because of the larger concentration gradient and driving force for mass transfer, which increases the number of dye molecules around each gram of the adsorbent and facilitates the uptake of all dye molecules. This behavior indicates that as adsorbent sites become saturated at higher dye concentrations, it is still able to adsorb more dye per unit mass. A similar pattern can be observed for both MO and MR. At the same time, differences in molecular size, charge and affinity for the carbon surface could influence specific adsorption behaviour of these two acids [30, 31].

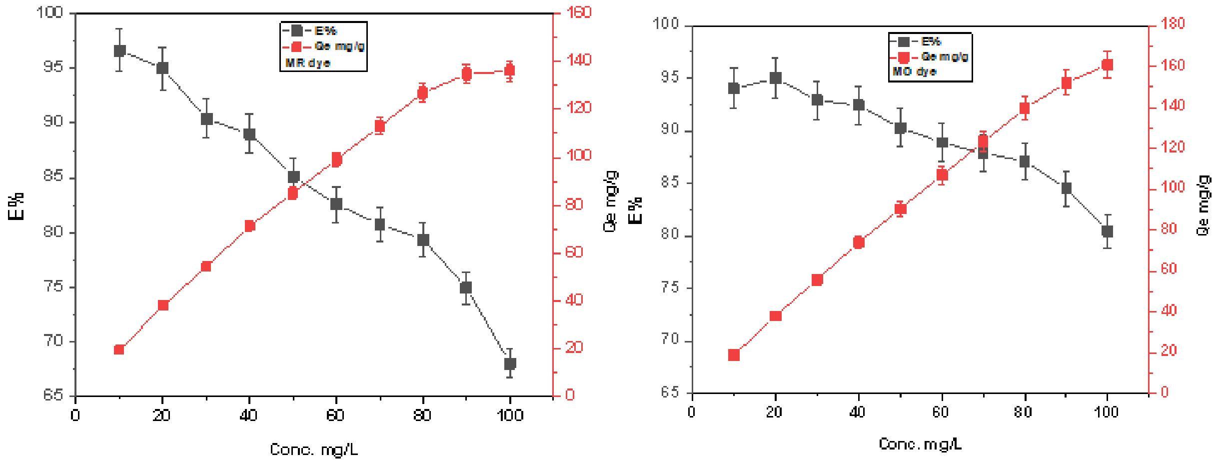

Figure 5. Effect of initial dye concentration on the adsorption of methyl orange (MO) and methyl red (MR) dyes

3.3. Influence of temperature

The effects of temperature on the adsorption of methyl red (MR) and methyl orange (MO) dyes from aqueous solution onto activated carbon obtained from corn cobs were investigated. The results indicated that as the temperature increased, the removal efficiency decreased for both dyes. This reduction suggests that the adsorption process of the dye on the surface of the carbon sample is exothermic and that increased temperatures weaken the interaction between the dye molecules and the carbon surface[32]. At higher temperatures, more thermal energy can further enhance the migration of dye molecules in solution, while breaking physical forces such as van der Waals forces and hydrogen bonds, which are essential for adsorption. In addition, the higher temperature can enhance desorption of the adsorbed dye molecules, and hence, decrease the overall removal percent. For both methyl red and methyl orange, the removal efficiency was slightly greater for methyl red than for methyl orange at the tested temperatures. This discrepancy could have originated from a better binding or stronger immobilization of MR molecules on the AC surface compared to those of MO, which might be due to differences in molecular size, structure, and charge distribution[33, 34]. The results showed that bio-based activated carbon is better suited for dye adsorption at lower temperatures, and MR is a better dye for adsorption than MO under the studied conditions. As shown in Figure 6.

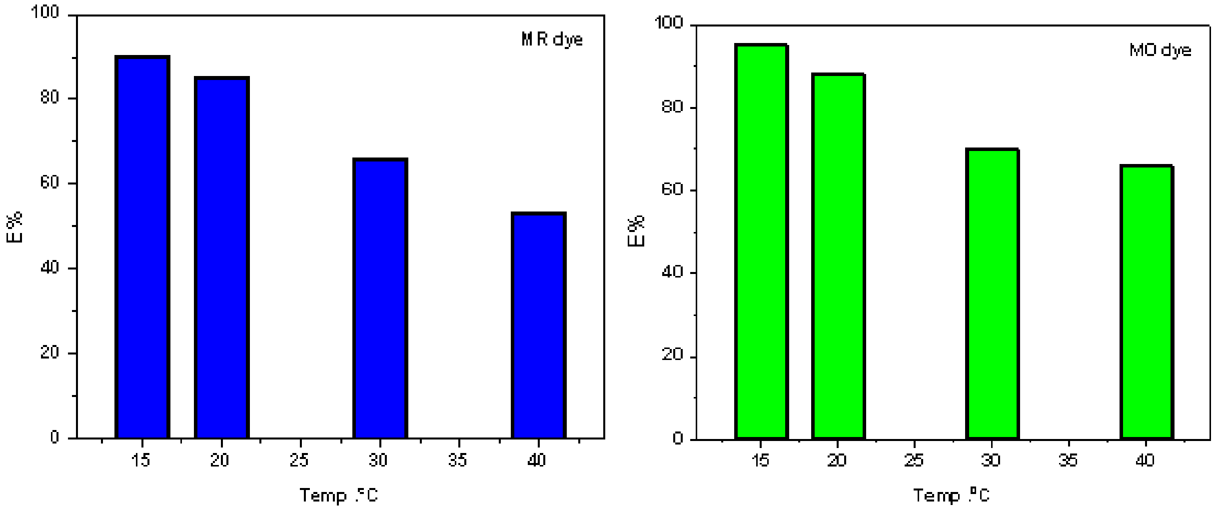

Figure 6. Influence of temperature on the efficiency of dye removal

Adsorption Isotherm

Langmuir Isotherm

The equilibrium uptake of methyl orange (MO) and methyl red (MR) on the activated carbon was modeled with the Langmuir isotherm, which assumes a homogeneous surface with energetically identical sites, single occupancy per site (monolayer coverage), and no lateral adsorbate–adsorbate interactions at constant temperature. Under these assumptions, once a dye molecule occupies a site, no further adsorption can occur at that site. The nonlinear Langmuir form is:

$$q_e = \frac{q_m K_L C_e}{1 + K_L C_e} \tag{3}$$

Freundlich Isotherm

The heterogeneous adsorption of MO and MR molecules at various locations with varying spatial energies of adsorption is described by the Freundlich isotherm model, as opposed to the Langmuir isotherm. Consequently, the exponential distribution of locations and adsorption energies affects the quantity of MO and MR adsorption on activated carbon. The nonlinear version of the Freundlich isotherm was obtained using Eq:**(4) .**

$$q_e = K_f C_e^{1/n} \tag{4}$$

The nonlinear connection shown in Figure 7 with the data from Table 1, 2 represents the Freundlich isotherm equilibrium constants KF and 1/n, which are related to the system's sorption capacity and sorption intensity and may be displayed as a function of Qe mg/g vs Ce mg/L . The isothermal models were assessed using the determination coefficient (R2). With a determination value of R^2 = 0.96894,0.988 the Frundlich isotherm therefore fits the continuous equilibrium of MO, and MR removal by AC, indicating multilayer physical type adsorption[35].

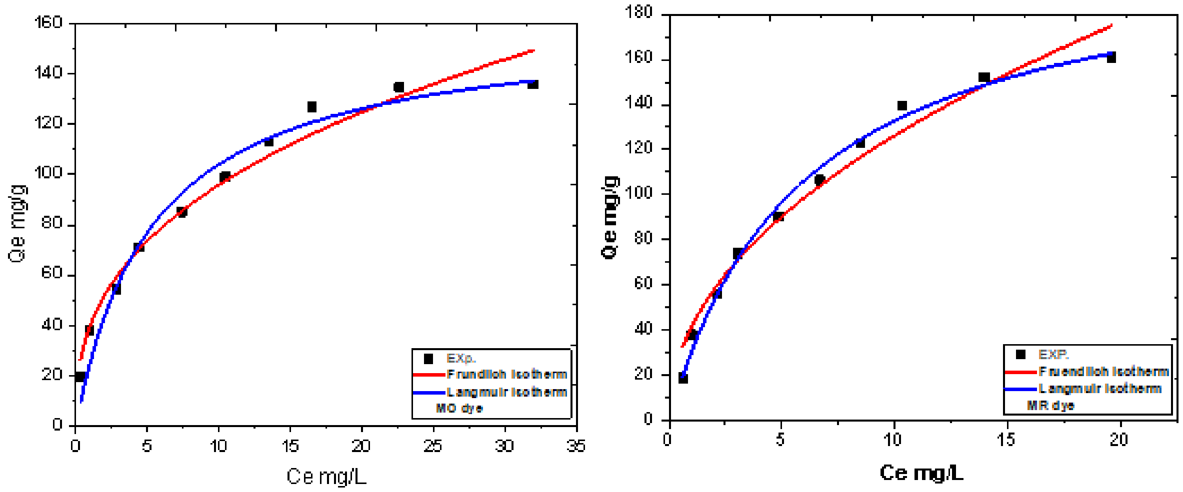

Figure 7. Adsorption isotherm nonlinear fit of adsorption of MO and MR dye onto activated carbon

Table 1. Different Factors of models for the adsorption study of MO dye onto activated carbon

	Activated carbon	
Temperature/ °c		25 °c
Freundlich isotherm	K_f	39.11 ± 0.222
	1/n	0.356 ± 0.044
	R^2	0.9681
Langmuir isotherm	Q_m (mg/g)	55.936 ± 12.22
	K_L (L/mg)	0.988 ± 0.022
	R^2	0.9277

Table 2. Different Factors of models for the adsorption study of MR dye onto activated carbon

	Activated Carbon	
Temperature/ °C		25 °C
Freundlich Isotherm	K_f	41.11 ± 0.311
	1/n	0.444 ± 0.022
	R^2	0.9681
Langmuir Isotherm	q_m (mg/g)	52212.22± 0.22
	K_L (L/mg)	0.988 0.655± 0.022
	R^2	0.9588

Thermodynamic adsorption

Since temperature has a major impact on adsorption capacity, determining the adsorption temperature is thought to be a crucial first step in differentiating between chemisorption and physisorption. In the experiments performed in this study, as the temperature rose, the adsorption removal effectiveness dropped. At 30 °C, the greatest adsorption capacity of the target dye, MO, was 110 mg/g. The effectiveness of dye removal was reduced when the solution temperature was raised from 15 °C to 40 °C. This suggests that the process of biosorption was exothermic. Thermodynamics relates to the conditions of equilibrium in physical and chemical processes throughout the adsorption process. Thermodynamic parameters are used to identify changes in an adsorption process's enthalpy (ΔH°), entropy (ΔS°), and Gibbs energy (ΔG°). It is possible to determine whether the adsorption phenomenon was endothermic or exothermic using the thermodynamic properties . The intercept and slope of the Van't Hoff plot are used to calculate the values of (ΔH°), (ΔS°), and (ΔG°). The following equations were used to determine the thermodynamic parameters .Table 3 displays the computed values of parameters (ΔG°), (ΔH°), and (ΔS°).[36]

$$K_e=\frac{(Q_{max})*Wt\,(gm)}{(C_e)*V(L)}\times 1000 \tag{3}$$

$$\Delta G = -RT \ln K_e \tag{4}$$

$$\Delta G = \Delta H - T\Delta S \tag{5}$$

$$\ln X_m = -\frac{\Delta H^{\circ}}{RT} + Cons. \tag{6}$$

Table 3. Thermodynamic Factors for MO dye adsorption on activated carbon

Activated carbon			
ΔH° (KJ/mol)	**ΔG° (kJ/mol)**	**ΔS° ($J.mol^{-1}.K^{-1}$)**	**Equilibrium constant**
10.875	-7403.41	**147.876**	23.25581
	-7951.93		26.16279
	-8728.85		31.97674

4. Conclusion

This study successfully demonstrated the potential of hydrochloric acid-activated carbon derived from corn cob biomass as an efficient and sustainable adsorbent for the removal of synthetic dyes from aqueous solutions. The prepared activated carbon exhibited favorable surface characteristics, including high surface area and well-developed porosity, as confirmed by SEM, and TEM analyses. The adsorption experiments revealed that several operational parameters—such as adsorbent dosage, dye concentration, and temperature—significantly influence dye removal efficiency. Among the tested dyes, methyl red (MR) showed superior adsorption performance compared to methyl orange (MO), which can be attributed to its smaller molecular size, stronger interaction with surface functional groups, and more favorable electrostatic and π–π stacking interactions. Increasing the adsorbent dose enhanced dye removal percentage due to the greater availability of active sites, while the adsorption capacity per unit mass (qe) decreased due to surface area overlap and particle aggregation at higher dosages. Overall, the findings support the feasibility of using agricultural waste materials, such as corn cobs, as low-cost precursors for producing activated carbon for wastewater treatment applications. The study contributes to sustainable environmental practices and encourages the valorization of biomass for pollution control.

Conflict of interest

The authors declare no conflict of interest

References

1. Sharma, A.K., et al., Environmentally benign approach for the efficient sequestration of methylene blue and coomassie brilliant blue using graphene oxide emended gelatin/؛خ-carrageenan hydrogels. International Journal of Biological Macromolecules, 2022. 219: p. 353-365: https://doi.org/10.1016/j.ijbiomac.2022.07.216.
2. Sourbh , T., Synthesis, characterization and adsorption studies of an acrylic acid-grafted sodium alginate-based TiO2 hydrogel nanocomposite. Adsorption Science & Technology, 2018. 36(1-2): p. 458–477.
3. Pathania, D., S. Sharma, and P. Singh, Removal of methylene blue by adsorption onto activated carbon developed from Ficus carica bast. Arabian Journal of Chemistry. 10: p. S1445-S1451.
4. Salleh, A., et al., Cationic and Anionic Dye Adsorption by Agricultural Solid Wastes: A Comprehensive Review. Desalination, 2011. 280: p. 1-13.
5. Rahul and R. Jindal, Efficient removal of toxic dyes malachite green and fuchsin acid from aqueous solutions using Pullulan/CMC hydrogel. Polymer, 2024. 307: p. 127203: https://doi.org/10.1016/j.polymer.2024.127203.
6. Rana, V.S. and N. Sharma, Adsorption profile of anionic and cationic dyes through Fe3O4 embedded oxidized Sterculia gum/Gelatin hybrid gel matrix. International Journal of Biological Macromolecules, 2023. 232: p. 123098: https://doi.org/10.1016/j.ijbiomac.2022.12.317.
7. Al-Gubury, H.Y., et al., Photcatalytic degradation n-undecane using coupled ZnO-Co2O3. International Journal of Chemical Sciences, 2015. 13(2): p. 863-874.
8. Salunkhe, B. and T.P. Schuman, Super-Adsorbent Hydrogels for Removal of Methylene Blue from Aqueous Solution: Dye Adsorption Isotherms, Kinetics, and Thermodynamic Properties. Macromol, 2021. 1(4): p. 256-275: https://doi.org/10.3390/macromol1040018.
9. Saeed, A., M. Sharif, and M. Iqbal, Application potential of grapefruit peel as dye sorbent: Kinetics, equilibrium and mechanism of crystal violet adsorption. Journal of Hazardous Materials, 2010. 179(1): p. 564-572 :https://doi.org/10.1016/j.jhazmat.2010.03.041.
10. Kareem, A., et al., Removal of methylene blue dye from aqueous solutions by using activated carbon/ureaformaldehyde composite resin as an adsorbent. International Journal of Chemical Sciences, 2016. 14(2): p. 635-648.
11. Al-Aidy, H. and E. Amdeha, Green adsorbents based on polyacrylic acid-acrylamide grafted starch hydrogels: the new approach for enhanced adsorption of malachite green dye from aqueous solution. International Journal of Environmental Analytical Chemistry, 2021. 101(15): p. 2796-2816: https://doi.org/10.1080/03067319.2020.1711896.
12. Thamer, B.M., F.A. Al-Aizari, and H.S. Abdo, Activated Carbon-Incorporated Tragacanth Gum Hydrogel Biocomposite: A Promising Adsorbent for Crystal Violet Dye Removal from Aqueous Solutions. Gels, 2023. 9(12).
13. Aljeboree, A.M., et al., Highly Reusable Nano Adsorbent Based on Clay-Incorporated Hydrogel Nanocomposite for Cationic Dye Adsorption. Journal of Inorganic and Organometallic Polymers and Materials, 2025. 35(2): p. 1165-1186.
14. Sharma, S., et al., Adsorption of cationic dyes onto carrageenan and itaconic acid-based superabsorbent hydrogel: Synthesis, characterization and isotherm analysis. Journal of Hazardous Materials, 2021. 421: p. 126729 :https://doi.org/10.1016/j.jhazmat.2021.126729.
15. Shirsath, S.R., et al., Ultrasonically prepared poly(acrylamide)-kaolin composite hydrogel for removal of crystal violet dye from wastewater. Journal of Environmental Chemical Engineering, 2015. 3(2): p. 1152-1162: https://doi.org/10.1016/j.jece.2015.04.016.
16. Zhou, Z., et al., Adsorption of food dyes from aqueous solution by glutaraldehyde cross-linked magnetic chitosan nanoparticles. Journal of Food Engineering, 2014. 126: p. 133-141: https://doi.org/10.1016/j.jfoodeng.2013.11.014.
17. Thamer, B.M., et al., Highly selective and reusable nanoadsorbent based on expansive clay-incorporated polymeric nanofibers for cationic dye adsorption in single and binary systems. Journal of Water Process Engineering, 2023. 54: p. 103918: https://doi.org/10.1016/j.jwpe.2023.103918.
18. Sadeghy, S., et al., Modeling and optimization of direct dyes removal from aqueous solutions using activated carbon produced from sesame shell waste. Scientific Reports, 2024. 14(1): p. 24867: https://doi.org/10.1038/s41598-024-76081-x.
19. Thamer, B.M., et al., In Situ Preparation of Novel Porous Nanocomposite Hydrogel as Effective Adsorbent for the Removal of Cationic Dyes from Polluted Water. Polymers, 2020. 12(12): p. 3002; https://doi.org/10.3390/polym12123002.
20. 20. Amjad, F., et al., A superabsorbent and pH-responsive copolymer-hydrogel based on glucomannans from Ocimum basilicum (sweet basil): A smart and non-toxic material for intelligent drug delivery. International Journal of Biological Macromolecules, 2025. 315: p. 144452.
21. Shen, Y., B. Li, and Z. Zhang, Super-efficient removal and adsorption mechanism of anionic dyes from water by magnetic amino acid-functionalized diatomite/yttrium alginate hybrid beads as an eco-friendly composite. Chemosphere, 2023. 336: p. 139233: https://doi.org/10.1016/j.chemosphere.2023.139233.

22. Aljeboree, A.M., et al., Preperation of sodium alginate-based SA-g-poly(ITA-co-VBS)/RC hydrogel nanocomposites: And their application towards dye adsorption. Arabian Journal of Chemistry, 2024. 17(3).
23. Zhao, Y., et al., Preparation of SA-g-(PAA-co-PDMC) polyampholytic superabsorbent polymer and its application to the anionic dye adsorption removal from effluents. Separation and Purification Technology, 2017. 188: p. 329-340: https://doi.org/10.1016/j.seppur.2017.07.044.
24. Aljeboree, A.M., et al., Optimization of swelling and mechanical behavior of novel pH-sensitive terpolymer biocomposite hydrogel based on activated carbon for removal brilliant blue dye from aqueous solution. Polymer Bulletin, 2024: p. https://doi.org/10.1007/s00289-024-05588-0.
25. Zoya, Z., A. Aisha, and S.A. Elham, Adsorption of methyl red on biogenic Ag@Fe nanocomposite adsorbent: Isotherms, kinetics and mechanisms. Journal of Molecular Liquids, 2019. 283: p. 287-298 :https://doi.org/10.1016/j.molliq.2019.03.030.
26. Chollom, M.N., et al., Comparison of response surface methods for the optimization of an upflow anaerobic sludge blanket for the treatment of slaughterhouse wastewater. Environmental Engineering Research, 2020. 25(1): p. 114-122.
27. Ullah, N., et al., Preparation and dye adsorption properties of activated carbon/clay/sodium alginate composite hydrogel membranes. RSC Advances, 2024. 14(1): p. 211-221.
28. Boztepe, C., et al., Synthesis and characterization of acrylamide-based copolymeric hydrogel–silver composites: Antimicrobial activities and inhibition kinetics against E. coli. International Journal of Polymeric Materials and Polymeric Biomaterials, 2017. 66(18): p. 934-942.
29. Tainara, V., Samantha E. S. ,Artifon, C. T. ,Pâmela B. V., Valter A. B. , Alexandre T. P.,, Chitosan-based hydrogels for the sorption of metals and dyes in water: isothermal, kinetic, and thermodynamic evaluations. Colloid and Polymer Science, 2021. 299: p. 649–662.
30. Aljeboree, A.M., et al., Hydrothermal synthesis of eco-friendly ZnO/CNT nanocomposite and efficient removal of Brilliant Green cationic dye. Results in Chemistry, 2024. 7: p. 101364: https://doi.org/10.1016/j.rechem.2024.101364.
31. Chien, S. and W. Clayton, Application of Elovich equation to the kinetics of phosphate release and sorption in soils. Soil Science Society of America Journal, 1980. 44(2): p. 265-268.
32. Shah, S.S., B. Ramos, and A.C. Teixeira Adsorptive Removal of Methylene Blue Dye Using Biodegradable Superabsorbent Hydrogel Polymer Composite Incorporated with Activated Charcoal. Water, 2022. 14, DOI: 10.3390/w14203313.
33. Aljeboree, A.M., et al., Highly Reusable Nano Adsorbent Based on Clay-Incorporated Hydrogel Nanocomposite for Cationic Dye Adsorption. Journal of Inorganic and Organometallic Polymers and Materials, 2025. 35(2): p. 1165-1186 : https://doi.org/10.1007/s10904-024-03344-5.
34. Dave, P.N., et al., Fabrication and characterization of a gum ghatti-cl-poly(N-isopropyl acrylamide-co-acrylic acid)/CoFe2O4 nanocomposite hydrogel for metformin hydrochloride drug removal from aqueous solution. Current Research in Green and Sustainable Chemistry, 2023. 6: p. 100349: https://doi.org/10.1016/j.crgsc.2022.100349.
35. Sultana, S., et al., Adsorption of Cu (II) ions from aquatic environment using pre-irradiated Ethylene Tetrafluoroethylene Film. Applied Chemical Engineering, 2024. 7(1).
36. Zhao, H., et al., Nickel particle/graphene composite as a new matrix-assisted laser de-sorption ionization mass spectrometry matrix and adsorbent for high performance mass spectrometry analysis of biological small molecules. Applied Chemical Engineering, 2022. 5(2): p. 45-56.